Supplementary Material

Molecular assembly with figure-of-eight nanohoop as a strategy for collection and stabilization of cyclo[18]carbon

*Zeyu Liu, *[a] Xia Wang, [a] Tian Lu, *[b] Jiaojiao Wang, [a] Xiufen Yan, [a] Yang Wu, [a] and Jingbo Xu*

[a]School of Environmental and Chemical Engineering, Jiangsu University of Science and Technology, Zhenjiang 212100, People's Republic of China

[b]Beijing Kein Research Center for Natural Sciences, Beijing 100022, People's Republic of China

Contents:

Section S1. Computational details

Due to the extremely unusual electronic structure of C_{18}, special attention should be paid to the selection of computing methods for it. Many theoretical studies have demonstrated that hybrid density functional containing more than 25% global Hartree-Fock (HF) exchange, such as M06-2X,[S1] or containing very high HF exchange at long-range region, such as ωB97XD,[S2] combined with at least 6-311G(d) basis set,[S3] can replicate its polyynic structure with alternating long and short bonds.[S4-S6] In contrast, it is generally accepted that the geometry of organic conjugated macrocycles is insensitive to the level of basis set. Therefore, we adopted the ωB97XD method combined with 6-311G(d) (for free and composited C_{18} ring) and 6-31G(d)[S7] (for other molecules and composited parts) basis sets to optimize all species discussed. The vibrational frequencies obtained at the same theoretical level were used to characterize the stationary point as energy minima.

Intermolecular interaction between C_{18} and OPP was evaluated using ωB97M-V[S8] functional in combination with def2-QZVPP basis set,[S9] because this level is able to accurately estimate interaction energy (E_{int}) for a wide variety of weakly interacting complexes.[S10] However, this calculation is too computationally demanding to handle the entire complexes C_{18}@OPP and $2C_{18}$@OPP. Considering that the interatomic interaction between C_{18} and OPP decays rapidly with distance, and that the morphology of the loop complexed with C_{18} is basically unaffected by another loop, the OPP was simplified to retain only one loop in the calculation of E_{int} (see **Fig. S1** for illustration). The binding enthalpy of C_{18}@OPP was evaluated as $\Delta H_b = E_{int} + \Delta H_b^{corr}$, where ΔH_b^{corr} is the variation of thermal correction to enthalpy during binding. ΔH_b^{corr} and entropy were calculated based on harmonic frequencies by Shermo code with Grimme's quasi-rigid-rotor harmonic oscillator model.[S11] The deformation energy of C_{18} and OPP representing the energy increase due to structure distortion during complexation were not considered explicitly, because their magnitudes are completely negligible, which can be learned from the discussion of the configuration superposition in the main text.

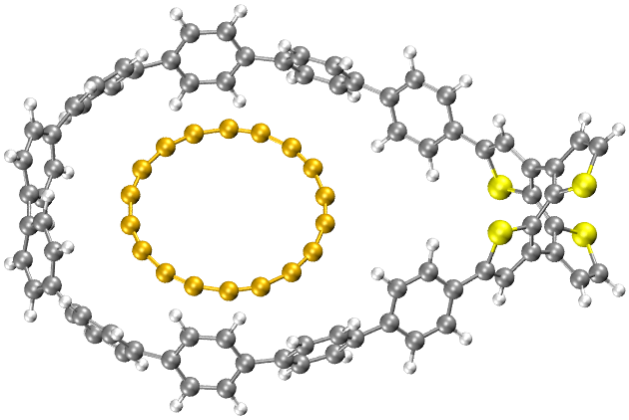

Fig. S1. Simplified model for calculations of interaction energy between C_{18} and OPP. One loop of OPP is removed and the truncated C-C bonds are saturated with hydrogens. Coordinates of all atoms except for the newly added hydrogens are in line with those in the C_{18}@OPP complex optimized at ωB97XD/6-311G(d)&6-31G(d) level.

In order to calculate binding energy between C_{18} and OPP at S_1 excited state, we optimized minimum structure of S_1 state of $2C_{18}$@OPP and OPP via time-dependent density functional theory (TD-DFT) using the same DFT functional and basis set as aforementioned ground-state calculations, and then the binding energy was calculated as

$$\Delta E_{\text{bind}}^{\text{S1}} = E[(\text{C}_{18}@\text{OPP})_{\text{S1,model}}] - E[(\text{OPP})_{\text{S1,model}}] - E[(\text{C}_{18})_{\text{S0}}]$$

where the first term at the right-hand side is the energy of C_{18}@OPP based on simplified model of optimized S_1 geometry of $2C_{18}$@OPP, the second term is the energy of OPP based on simplified model of optimized S_1 geometry of OPP, and the third term is the energy of C_{18} optimized at its isolated geometry. The energies were evaluated using ωB97M-V/def2-QZVPP level. Because the S_1 state of $2C_{18}$@OPP fully corresponds to a local excitation at the central linker of OPP, consideration of excitation of C_{18} is completely avoided. Also due to this reason and only the loop regions of OPP have notable interaction with C_{18}, it is fully reasonable to calculate the binding energy between C_{18} and OPP in S_1 state via ground-state theoretical method (ωB97M-V). So, the binding energy between C_{18} and OPP at ground state was calculated in the same way, except that all geometries were optimized at ground state.

The excitation energies and oscillator strengths were calculated with the TD-DFT using PBE38 functional with the same choice of basis sets as the geometric

optimization. The PBE38 is a hybrid density functional built based on the very popular PBE0[S12] by increasing its HF exchange from 25% to 3/8 (37.5%). We employ it because it is shown that PBE38 is quite satisfactory for studying excited states for organic systems with extensive π-conjugation like OPP,[S13] and its relatively high HF exchange guarantees that electronic structure of C_{18} can be correctly represented. All quantum chemistry calculations were carried out by Gaussian 16 (A.03) software,[S14] except that *ω*B97M-V single-point calculations were conducted using ORCA 5.0.3 program.[S15]

MD simulation was realized by GROMACS 2018.8 program[S16] basically based on general amber force field (GAFF). [S17] Specifically, for representing C_{18}, c1 atom type (suitable for *sp*-hybridized carbon) was assigned for the carbons, and c1-c1-c1 angle parameter was employed. Parameters of long and short C-C bonds in C_{18} were respectively generated by modified Seminario method[S18] based on Hessian matrix at *ω*B97XD/def2-TZVP level. For representing OPP, proper GAFF atom types and corresponding bond, angle, and dihedral parameters were assigned. However, we found the rigid structure of cyclooctatetrathiophene linker region between the two loops of OPP cannot be well maintained via GAFF bonded parameters during MD simulation, therefore the bonded parameters related to this region were produced by modified Seminario method based on Hessian matrix at *ω*B97XD/6-311G(d) level. The assignment of GAFF parameter, the modified Seminario calculation, and the generation of final GROMACS topology files were finished by Sobtop code. [S19]

We superimposed the structure of $2C_{18}$@OPP calculated by FF method with that optimized by DFT, and the result shows that the geometric structure of the supramolecular complex obtained by the two methods is not significantly different (**Fig. S2**). The comparison results of structure and energy jointly demonstrate the reliability of the molecular FF and computational strategy we have chosen. Energy decomposition based on GAFF was also employed to study intermolecular interaction for $2C_{18}$@OPP. Only van der Waals (vdW) interaction was taken into account because atomic charges of C_{18} are all close to zero and thus electrostatic interaction cannot be represented. The interaction energy between each pair of C_{18} and OPP derived in this way is -26.0 kcal/mol, which is close to the *ω*B97M-V/def2-QZVPP result of -20.3 kcal/mol.

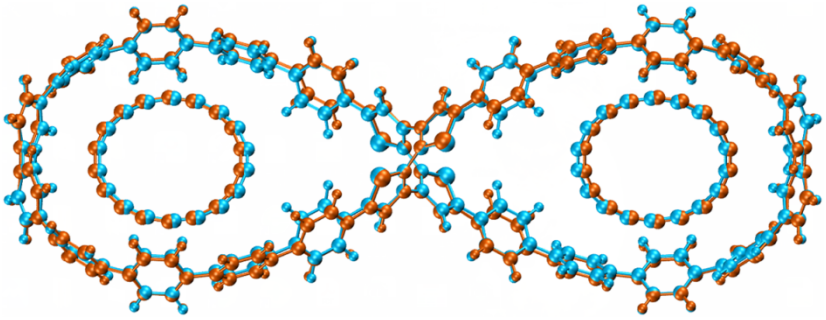

Fig. S2. Conformational superpositions of the minimum structure of $2C_{18}$@OPP optimized by DFT with that calculated by FF method. Color code: blue, DFT-optimized structure; orange, FF-calculated structure.

To simulate the formation of $2C_{18}$@OPP, we constructed a box containing a large vacuum region by extending 4 nm around the OPP, and then inserted two C_{18} molecules at random positions with arbitrary orientations. MD simulation for 2 ns was performed at a maintaining temperature of 300 K via velocity rescale thermostat.[S20] Initial atomic velocities were randomly generated according to Maxwell distribution corresponding to actual simulation temperature. The periodic boundary condition was adopted to ensure that C_{18} could re-enter the box when it moves out. The translational and angular motions of the OPP were eliminated during the simulation, thus keeping the OPP always centered in the box. In the MD simulation, time step was set to 2 fs and trajectory snapshots were saved every 0.2 ps. Because atomic charges of C_{18} are all zero due to its structure symmetry, electrostatic interaction was not taken into account in the simulation. Ignoring it is acceptable since the C_{18}···OPP interaction is dominated by vdW effect, as discussed in the main text.

In our five 5 ns MD simulations of C_{18}@OPP at each temperature of 100, 200, 300, 400, and 500 K, as well as a 20 ns simulation at 500, 600, and 800 K respectively, the employed simulation conditions are the same as those described above.

Electrostatic potential (ESP), van der Waals (vdW) potential, Mayer bond order, and independent gradient model based on Hirshfeld partition (IGMH) analyses were all finished by Multiwfn 3.8(dev) code.[S21] All isosurface and molecular structure maps were rendered by VMD software.[S22]

Notes and references

(S1) Zhao, Y.; Truhlar, D. G. *Theor. Chem. Acc.* **2008**, *120*, 215–241.

(S2) Chai, J. D.; Head-Gordon, M. *Phys. Chem. Chem. Phys.* **2008**, *10*, 6615–6620.

(S3) Hehre, W. J.; Ditchfield, R.; Pople, J. A. *J. Chem. Phys.* **1972**, *56*, 2257.

(S4) Liu, Z.; Lu, T.; Chen, Q. *Carbon* **2020**, *165*, 468–475.

(S5) Baryshnikov, G. V.; Valiev, R. R.; Kuklin, A. V.; Sundholm, D.; Ågren, H. *J. Phys. Chem. Lett*. **2019**, *10*, 6701–6705.

(S6) Liu, Z.; Lu, T.; Chen, Q. *J. Mol. Model.* **2021**, *27*, 42.

(S7) Krishnan, R.; Binkley, J. S.; Seeger, R.; Pople, J. A. *J. Chem. Phys.* **1980**, *72*, 650.

(S8) Mardirossian, N.; Head-Gordon, M. *J. Chem. Phys.* **2016**, *144*, 214110.

(S9) Weigend, F.; Ahlrichs, R. *Phys. Chem. Chem. Phys.* **2005**, *7*, 3297–3305.

(S10) Mardirossian, N.; Head-Gordon, M. *Mol. Phys.* **2017**, *115*, 2315–2372.

(S11) Lu, T.; Chen, Q. *Comput. Theor. Chem.* **2021**, *1200*, 113249.

(S12) Perdew, J. P.; Burke, K.; Ernzerhof, M. *Phys. Rev. Lett.* **1996**, *77*, 3865–3868.

(S13) Goerigk, L.; Grimme, S. *J. Chem. Phys.* **2010**, *132*, 184103.

(S14) Frisch, M. J.; Trucks, G. W.; Schlegel, H. B.; Scuseria, G. E.; Robb, M. A.; Cheeseman, J. R.; et al. *Gaussian 16,* revision A.03; Gaussian, Inc.: Wallingford, CT, **2016**.

(S15) Frank Neese. *WIREs: Comp. Mol. Sci.* **2022**, e1606.

(S16) Abrahama, M. J.; Murtola, T.; Schulz, R.; Páll, S.; Smith, J. C.; Hess, B.; Lindahl, E. *SoftwareX* **2015**, *1–2*, 19–25.

(S17) Wang, J.; Wolf, R. M.; Caldwell, J. W.; Kollman, P. A.; Case, D. A. *J. Comput. Chem.* **2004***, 25*, 1157–1174.

(S18) Allen, A. E. A.; Payne, M. C.; Cole, D. J. *J. Chem. Theory Comput.* **2018**, *14*, 274−281.

(S19) Lu, T. http://sobereva.com/soft/Sobtop (accessed on May 1, **2022**).

(S20) Bussi, G.; Donadio, D.; Parrinello, M. *J. Chem. Phys.***2007**, *126*, 014101.

(S21) Lu, T.; Chen, F. *J. Comput. Chem.* **2012**, *33*, 580–592.

(S22) Humphrey, W.; Dalke, A.; Schulten, K. *J. Mol. Graphics.* **1996**, *14*, 33–38.

Section S2. Detailed information about the geometric characters of C_{18}@OPP and $2C_{18}$@OPP

The orientation of guest C_{18} in the complexes almost coincides with the plane of the loop containing it, and the included angle is only slightly greater than 2.0º (**Table S1**). The angle between two loops of the host OPP in two complexes still remains about 70.0º as that in its free state, making the dihedral angle between two guests C_{18} in $2C_{18}$@OPP as high as about 65.0º. It is also found that the OPP is separated from the encapsulated C_{18} by a distance of 3.8 Å in C_{18}@OPP and $2C_{18}$@OPP, which just between the corresponding values of C_{70}@[10]CPP (3.4–3.8 Å) and C_{70}@[11]CPP (3.8–4.2 Å) and is close to the distance maintained by van der Waals (vdW) interaction between graphite sheets (3.4 Å).[S23] Therefore, there should be a considerable degree of vdW attraction between C_{18} and OPP in the complexes.

Table S1 Included angle between average planes of each part in complexes C_{18}@OPP and $2C_{18}$@OPP. The values are given in º.

	loop-1/loop-2	C_{18}-1/loop-1	C_{18}-2/loop-2	C_{18}-1/C_{18}-2
OPP	70.39	/	/	/
C_{18}@OPP	69.61	2.18	/	/
$2C_{18}$@OPP	68.92	2.11	2.11	64.70

Notes and references

(S23) Yuan, K.; Guo, Y. J.; Zhao, X. *J. Phys. Chem. C* **2015**, *119*, 5168−5179.

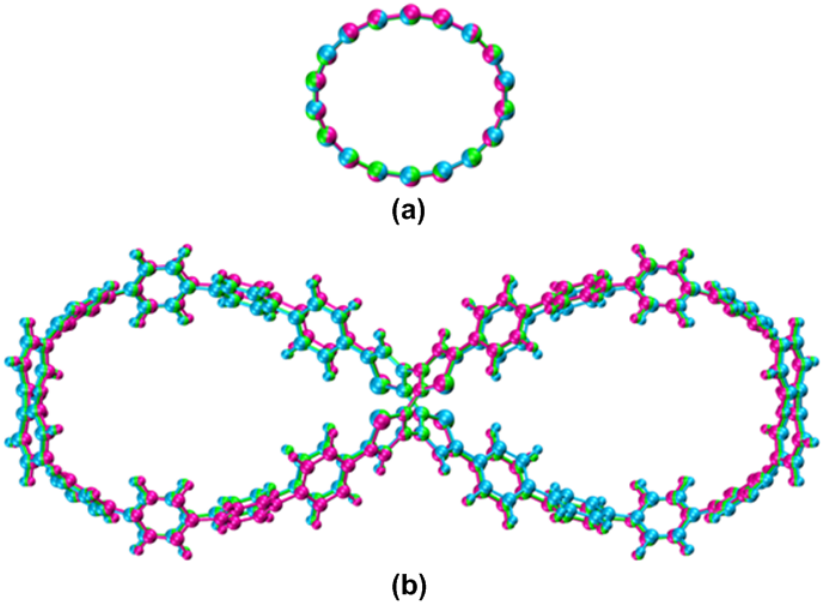

Fig. S3. Conformational superpositions of the free and composite states of (a) C_{18} ring and (b) OPP macrocycle. Color code: red, free host and guest molecules; green, host and guest moieties of C_{18}@OPP; blue, host and guest moieties of $2C_{18}$@OPP.

Table S2 Natural population charges of each part in complexes C_{18}@OPP and $2C_{18}$@OPP. The values are given in *e*.

	C_{18}-1	C_{18}-2	loop-1	loop-2
C_{18}@OPP	-0.03	/	0.03	0.00
$2C_{18}$@OPP	-0.03	-0.03	0.03	0.03

Section S3. Spectral characteristics of complexes C_{18}@OPP and $2C_{18}$@OPP

The IR spectroscopies of OPP, C_{18}@OPP, and $2C_{18}$@OPP appear similar in most regions (**Fig. S4(a)**), but there are three significant differences: (1) The introduction of C_{18} does not affect the wavenumber of the very strong IR absorption at 798.1 cm^{-1}, but there is a conspicuous enhancement of the absorption intensity with the addition of C_{18}. (2) The addition of C_{18} introduces a remarkable IR absorption at 379.6 cm^{-1}, and the more C_{18} is bound the stronger the spectroscopic intensity at this wavenumber. This absorption was observed to come entirely from the in-plane C-C-C bending vibrations of the C_{18} bound in loops. (3) The complexation of C_{18} with OPP also leads to a detectable absorption at 2122.0 cm^{-1}, which we found to be caused by the C-C bond stretching vibrations of the C_{18} ring.

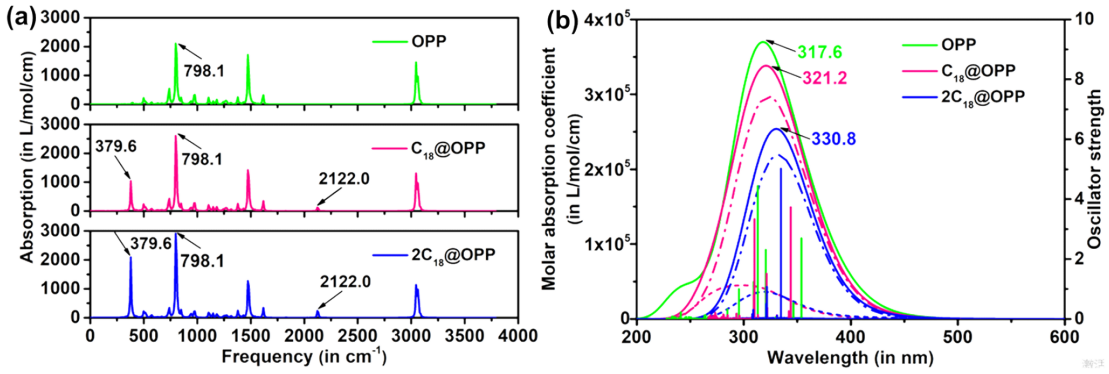

Fig. S4. (a) IR spectroscopy and (b) UV-Vis spectrum of OPP, C_{18}@OPP, and $2C_{18}$@OPP. The Lorentz and Gaussian functions with half-width at half height of 5.0 and 3000.0 cm^{-1} were employed for broadening the theoretical data as IR spectroscopy and UV-Vis spectrum, respectively. A fundamental scale factor of 0.949 was applied for all vibrational frequencies. The dash-dot and short-dash curves represent CTSs caused by electron transition within OPP and that from OPP to C_{18}, respectively, and other forms of electron excitation, that is, those from C_{18} to OPP and within C_{18}, are almost undetectable.

The excitation energies and oscillator strengths of the first 100 low-lying excited states of OPP, C_{18}@OPP, and $2C_{18}$@OPP were calculated, and the simulated UV-Vis spectra were plotted accordingly (**Fig. S4(b)**). The results of vertical excitation show that the only absorption of nanoring OPP centered at 317.6 nm is reasonably consistent with the experimental observation (342.0 nm).[S24] A slight red-shift in absorption bands is observed with a significant reduction in absorption intensity after

the complexation of host and guest molecules. Importantly, the electronic absorption spectra of complexes C_{18}@OPP and $2C_{18}$@OPP with different numbers of guest show distinctive characteristics, that is, the maximum absorption peak of $2C_{18}$@OPP with one more guest seems to have more red-shift and weaker intensity. As can be seen from charge-transfer spectrum (CTS) analysis proposed by us (see Supplementary Material of reference S25 for details), the absorption spectra of the two complexes are almost entirely derived from the electron redistribution within OPP and the charge transfer from OPP to C_{18}. So, the C_{18} plays a certain role in the electron excitation of the complexes, which is the fundamental reason why complexation makes the UV-Vis spectrum of the system change notably.

Notes and references

(S24) Zhan, L.; Dai, C.; Zhang, G.; Zhu, J.; Zhang, S.; Wang, H.; Zeng, Y; Tung, C-H; Wu, L-Z; Cong, H. *Angew. Chem. Int. Ed.* **2022**, *61*, e202113334.

(S25) Z. Liu, X. Wang, T. Lu, A. Yuan, X. Yan, *Carbon* **2022**, *187*, 78–85.

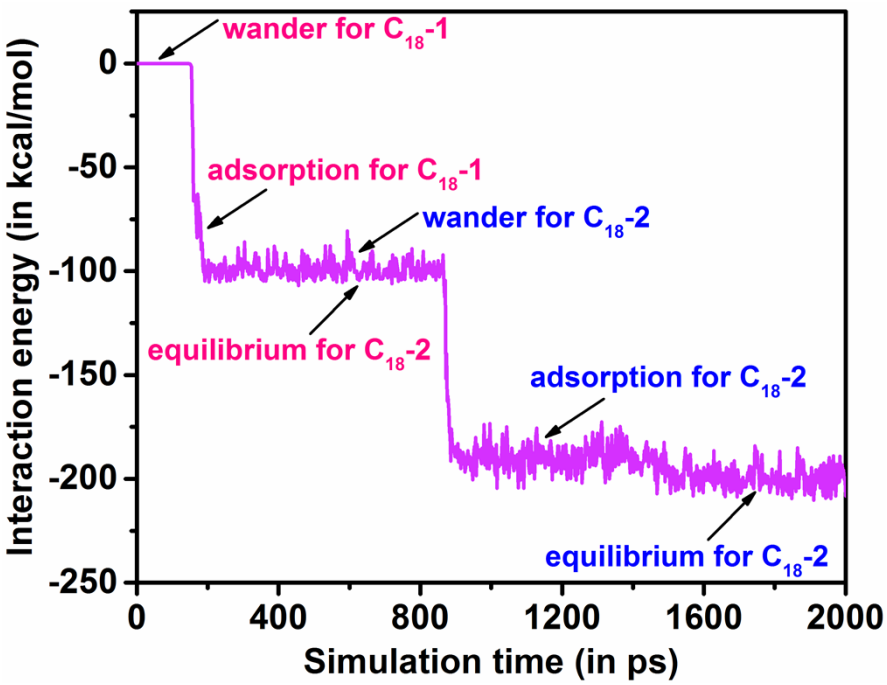

Fig. S5. Interaction energy between C_{18} and OPP during simulation of spontaneous entrance of two C_{18} into OPP.

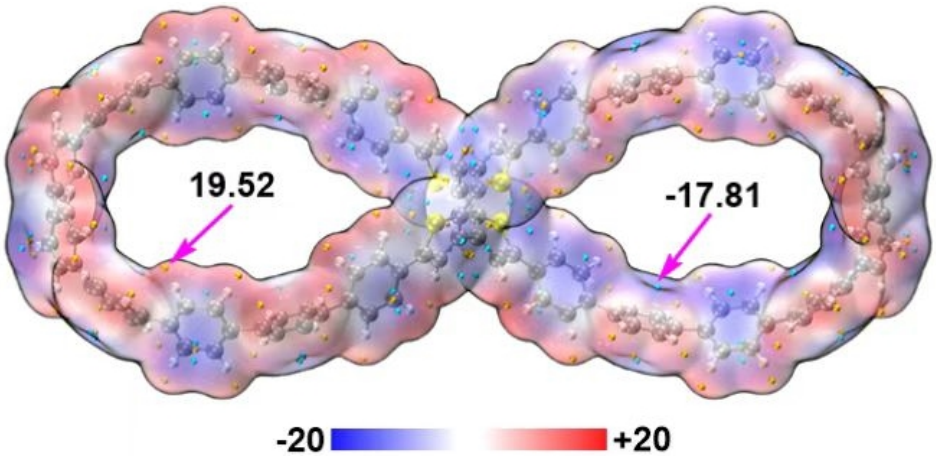

Fig. S6. ESP colored vdW surface map of the OPP. Values of selected ESP minima and maxima on the surface are labelled. The labels and color scale are given in kcal/mol/e.

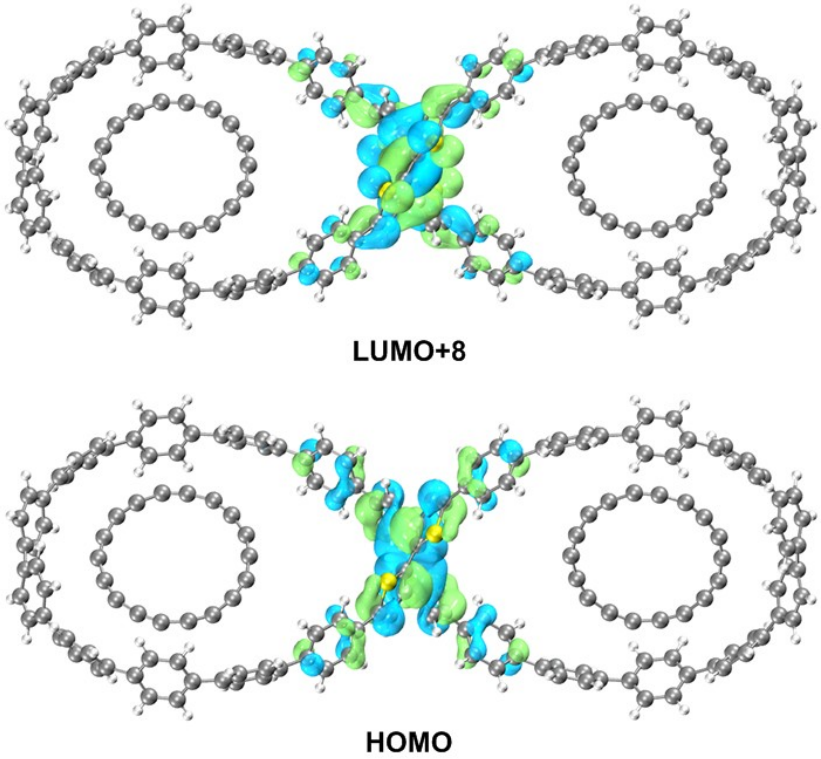

Fig. S7. Isosurface map of HOMO and LUMO+8 of $2C_{18}$@OPP under its S_1 state structure with isovalue of 0.02 a.u.

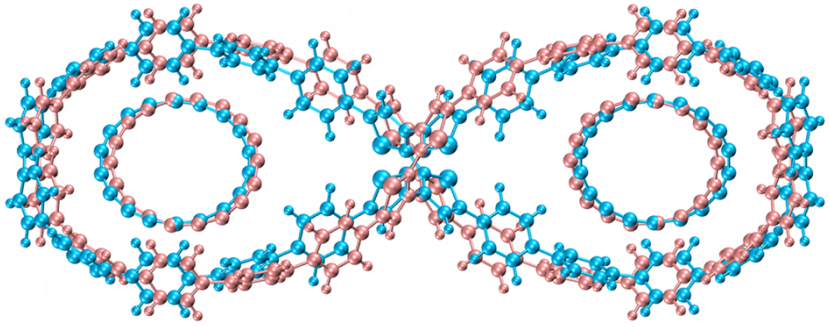

Fig. S8. Conformational superpositions of the minimum structure of the S_0 and S_1 states of $2C_{18}$@OPP. Color code: blue, the S0 state structure; pink, the S1 state structure.

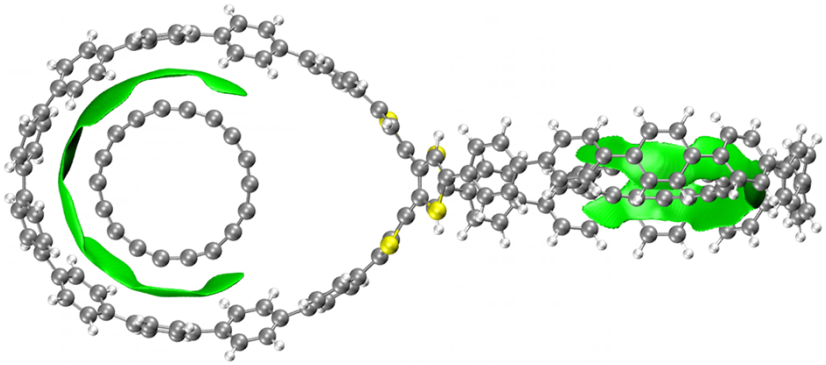

Fig. S9. Isosurface map of IGMH of S_1 state of $2C_{18}$@OPP with δg^{inter} isovalue of 0.002 a.u.